Inorg. Chem. **2006**, *45*, 4352–4358

The 136-Atom Structure of ZrP_2O_7 and HfP_2O_7 from Powder Diffraction Data

Graham W. Stinton, Matthew R. Hampson, and John S. O. Evans*

Department of Chemistry, Science Laboratories, University of Durham, South Road, Durham, DH1 3LE, U.K.

Received January 5, 2006

There has been considerable debate in the literature about the true room-temperature structure of ZrP_2O_7 and related materials. In this article we describe how a combination of information from solid-state ^{31}P NMR and powder diffraction data can be used to determine the structure of this 136 unique-atom material. The structure has been solved using a combination of simulated annealing and Rietveld refinement performed simultaneously on X-ray and neutron diffraction data. Despite the close to cubic metric symmetry of the material, we show how its true orthorhombic structure (space group *Pbca*) can be refined to a high degree of precision.

Introduction

ZrP_2O_7 is one of the most widely studied members of the pseudocubic AM_2O_7 family of materials (A = Si, Ge, Sn, Pb, Ti, Zr, Hf, Mo, W, Re, Ce, U, etc.; M = P, V, As)[1−14] One reason for interest in these materials is that they display unusual thermal expansion properties. ZrP_2O_7 shows positive thermal expansion up to around 566 K followed by low thermal expansion. ZrV_2O_7 shows negative thermal expansion above 375 K. Solid solutions of the form $ZrP_{2-x}V_xO_7$ have been shown to display negative thermal expansion down to room temperature.[9] A knowledge of the detailed structure of these materials is crucial in understanding their thermal expansion properties.

The ideal structure of AM_2O_7 materials is shown in Figure 1 and contains ZrO_6 octahedra which link to three of the corners of PO_4 tetrahedra; the fourth corner of each tetrahedron links to another tetrahedron to form P_2O_7 pyrophosphate groups. The structure can be likened to that of NaCl with ZrO_6 octahedra occupying the Na^+ positions and P_2O_7 groups occupying the Cl^- positions. In this ideal structure (which is believed to be the structure at high temperature), P_2O_7 groups lie along the main body diagonal of the cubic unit cell (space group $Pa\bar{3}$) and are therefore required to have 180° bond angles by symmetry, a situation which is energetically unfavorable. There is thus an energetic driving force at low temperature for P−O−P bonds to bend and lower the symmetry of the material, and it has long been known that at room temperature many AM_2O_7 materials adopt a superstructure in which the cell dimensions are tripled in all directions. For many years this superstructure was believed to have cubic symmetry and descriptions of the low-temperature (LT) ZrP_2O_7 structure have been published, albeit with bond distances and distortions of the polyhedral groups which are chemically unreasonable.[6] Recently a variety of evidence has appeared that suggests that many of these materials do not have cubic symmetry at room temperature. Peak splittings in powder diffraction patterns of GeP_2O_7 suggest it has monoclinic or triclinic symmetry.[15] SnP_2O_7 has been shown by ^{31}P NMR to have monoclinic symmetry with space group $P2_1$ or Pc.[16] One of us has shown using electron diffraction that the symmetry of ZrP_2O_7 is

* To whom correspondence should be addressed. E-mail: john.evans@durham.ac.uk. Phone: 44-191-3342093. Fax: 44-191-3844737.

(1) Krogh Andersen, A. M.; Norby, P. *Acta Crystallogr., Sect. B* **2000**, *56*, 618−625.
(2) Carlson, S.; Krogh Andersen, A. M. *J. Appl. Crystallogr.* **2001**, *34*, 7−12.
(3) Chaunac, M. *Bull. Soc. Chim. Fr.* **1971**, 424.
(4) Hagman, L.-O.; Kierkegaard, P. *Acta Chem. Scand.* **1969**, *23*, 327.
(5) Inomata, Y.; Inomata, T.; Moriwaki, T. *Spectrochim. Acta, Part A* **1980**, *36*, 839.
(6) Khosrovani, N.; Korthuis, V.; Sleight, A. W.; Vogt, T. *Inorg. Chem.* **1996**, *35*, 485.
(7) Kim, C. H.; Yim, H. S. *Solid State Commun.* **1999**, *110*, 1372.
(8) King, I. J.; Fayon, F.; Massiot, D.; Harris, R. K.; Evans, J. S. O. *Chem. Commun.* **2001**, 1766.
(9) Korthuis, V.; Khosrovani, N.; Sleight, A. W.; Roberts, N.; Dupree, R.; Warren, W. W. *Chem. Mater.* **1995**, *7*, 412.
(10) Levi, G. R.; Peyronel, G. *Z. Kristallogr.* **1935**, *92*, 190.
(11) Ota, T.; Yamai, I. *J. Mater. Sci.* **1987**, *22*, 3762.
(12) Seo, D. K.; Whangbo, M. H. *J. Solid State Chem.* **1997**, *129*, 160.
(13) Vollenkle, H.; Nowotny, H.; Wittman, A. *Monatsh. Chem.* **1963**, *94*, 956.
(14) Withers, R. L.; Tabira, Y.; Evans, J. S. O.; King, I. J.; Sleight, A. W. *J. Solid State Chem.* **2001**, *157*, 186.
(15) Losilla, E. R.; Cabeza, A.; Bruque, S.; Aranda, M. A. G.; Sanz, J.; Iglesias, J. E.; Alonso, J. A. *J. Solid State Chem.* **2001**, *156*, 213.
(16) Fayon, F.; King, I. J.; Harris, R. K.; Gover, R. K. B.; Evans, J. S. O.; Massiot, D. *Chem. Mater.* **2003**, *15*, 2234.

10.1021/ic060016b CCC: $33.50
Published on Web 04/26/2006

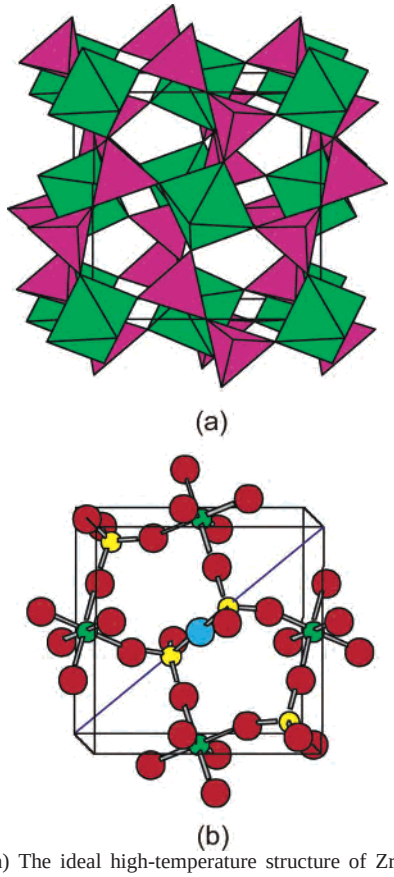

Figure 1. (a) The ideal high-temperature structure of ZrP_2O_7 contains corner sharing ZrO_6 octahedra and PO_4 tetrahedra; PO_4 tetrahedra share corners to form P_2O_7 pyrophospate groups. In the ideal structure P−O−P bonds are required by symmetry to be linear. (b) A ball and stick view of part of the structure emphasizing one P_2O_7 group is shown.

consistent with either space group $Pa\bar{3}$ or *Pbca*.[14] Two-dimensional ^{31}P solid-state NMR experiments have shown definitively that there are 27 distinct P sites in the unit cell arranged such that there are 13 $O_3P_a-O-P_bO_3$ groups in which the P_a and P_b atoms are crystallographically independent and 1 group in which the P_a and P_b atoms are related by symmetry. This allowed the space group of the material to be uniquely defined as *Pbca*, which means that, if crystallographically ordered, the one $O_3P_a-O-P_aO_3$ group has its oxygen atom formally lying on an inversion center.[8]

Given the space group symmetry of *Pbca*, the true structure of LT ZrP_2O_7 is necessarily complex and must contain 136 crystallographically unique atoms in the asymmetric unit. Owing to a first order phase transition which occurs in the material at around 566 K, single crystals have not been available, and structural work has had to be performed using powder diffraction data. Analysis of the powder data is further complicated by the fact that no peak splitting can be observed in samples we have prepared by high-temperature routes to indicate the lowering of symmetry from cubic to orthorhombic. In this paper we describe how, despite these limitations and the complexity of the material, it is possible to determine its full three-dimensional structure using powder diffraction data. To achieve this, we have used direct space structure solution methods applied simultaneously to X-ray and neutron diffraction data since X-ray data are sensitive to the positions of the heavy Zr and P sites, whereas neutron data are more sensitive to oxygen positions. We describe in this paper the methodology used and results obtained. Following completion of this structure solution, we became aware of the work of Birkedal et al. who have been able to prepare single crystals below the phase transition temperature using solution based methods and have determined the structure using single-crystal synchrotron diffraction.[17] Birkedal et al. have kindly supplied the coordinates they obtained, which allows valuable insight into the precision with which a structure this complex can be determined from powder data. This allows us to benchmark our techniques and judge their power for other cases where single crystals are not available. We note that single-crystal coordinates were only supplied after our structural work was complete and that no significant changes to our refinement methodology/model were made after their receipt.

Experimental Section

Synthesis. ZrP_2O_7 was synthesized using an adaptation of literature routes.[18,19] A 2:1 molar ratio of $ZrOCl_2 \cdot nH_2O$ (n determined thermogravimetrically to be 6.91) (Alfa, 99.985%) and phosphoric acid were mixed in a Pt crucible and allowed to stand at room temperature for 2 h. The sample was then heated at 5 K/min to 623 K, held at temperature for 1 h, cooled to room temperature, and crushed. The white sample was then washed/centrifuged with four batches of distilled water, dried at 453 K, and warmed at 3 K/h to 1023 K for 12 h. The sample was then ground and heated to 1273 K for 12 h and cooled to room temperature at 5 K/h. Powder diffraction suggested the sample was phase pure. DSC measurements on this sample of ZrP_2O_7 gave a phase transition temperature from the low- to high-temperature form of 566 K on warming and 561 K on cooling. Laboratory variable temperature X-ray diffraction studies on the same sample indicated the same phase transition temperature within experimental error. HfP_2O_7 was prepared by an analogous route.

Powder Diffraction Data. Neutron diffraction data were collected using the high-resolution powder diffractometer (HRPD) at the ISIS pulsed neutron source of the Rutherford Appleton Laboratory, U.K. Data were collected at room temperature using an 11 g sample loaded in a 15 mm cylindrical V can. Data from the backscattering bank of detectors were used for the refinements and were measured from 0.705 to 2.364 Å. Synchrotron X-ray diffraction data were collected at beam line X7A of the National Synchrotron Light Source at Brookhaven National Laboratory. Data were collected from 2 to 67.06° 2θ using a wavelength of $\lambda = 0.8013$ Å selected with a Ge(111) channel cut crystal monochromator and a step size of 0.01° on a flat plate sample using a multiwire position sensitive detector. Neutron diffraction data on a 0.56 g sample of HfP_2O_7 were collected using the ISIS GEM diffractometer, and X-ray data were collected using a Bruker d8 advanced diffractometer equipped with a Cu tube, Ge(111) incident beam monochromator, and M-Braun PSD from 10 to 120° 2θ.

Room-temperature cell parameters of ZrP_2O_7 and HfP_2O_7 were determined using laboratory powder diffraction data recorded on a Siemens d5000 diffractometer equipped with a Cu tube, graphite

(17) Birkedal, H.; Krogh Andersen, A. M.; Arakcheeva, A.; Chapuis, G.; Norby, P.; Pattison, P. *Inorg. Chem.* **2006**, *45*, 4346−4351.
(18) Harrison, D. E.; McKinstry, H. A.; Hummel, F. A. *J. Am. Ceram. Soc.* **1954**, *37*, 277.
(19) Huang, C. H.; Knop, O.; Othen, D. A.; Woodhams, F. W.; Howie, R. A. *Can. J. Chem.* **1975**, *53*, 79.

diffracted beam monochromator, and scintillation counter using a silicon ($a = 5.431\ 19$ Å) internal standard. Cubic subcell parameters of $a = 8.2465(3)$ and $a = 8.2147(1)$ Å respectively, were obtained. Synchrotron and neutron wavelengths and instrumental constants were calibrated using these value for $^1/_3$(vol$^{1/3}$) of the true tripled orthorhombic cell.

All calculations for structure solution and structure refinement were performed using the Topas Academic software suite written by Alan Coelho.[20] For combined refinements, data were weighted so X-ray and neutron patterns gave an approximately equal contribution to the overall weighted profile *R*-factor, R_{wp}. During structure solution with rigid bodies P−O(−P) bond lengths were defined in terms of the P−O−P bond angle (ang$_{P-O-P}$) using data extracted from the structure of TiP_2O_7;[21] that is,

$$d_{P-O}\,(\text{Å}) = 1.5396 + (2.619 \times 10^{-3})\text{ang} - (6.9732 \times 10^{-5})\text{ang}^2 + (7.8437 \times 10^{-7})\text{ang}^3$$

where ang = 180° − ang$_{P-O-P}$. During free atomic refinement, bond distance restraints of 2.0695 for Zr−O (derived from published Zr bond valence parameters[22,23]), 1.5000 for P−O(−Zr), and 1.5775 for P−O(−P) bond distances (derived from the 84 PO_4 tetrahedra in the structure of $Mo_2P_4O_{15}$[24]) were used. Bond angles within ZrO_6 octahedra and PO_4 tetrahedra were restrained to values of 90/180 and 109.5°.

Final Rietveld refinement of the ZrP_2O_7 superstructure was performed using neutron and X-ray data sets. A total of 446 parameters were refined: 37 instrumental/histogram terms and 409 structural parameters. For the neutron data, six background parameters (coefficients of a Chebychev polynomial), a scale factor, four peak shape parameters, and three instrument calibration constants were refined; for X-ray data, 13 background parameters, a scale factor, six peak shape parameters, a peak asymmetry correction, an absorption correction, and a zero point correction were refined. Structural parameters were three cell parameters, 402 coordinates, and four isotropic displacement parameters (Zr/P/O/bridging O's equated).

Rietveld refinement of the HfP_2O_7 superstructure was performed using GEM 90° and backscattering data banks and laboratory X-ray data. Equivalent restraints to those for ZrP_2O_7 were applied. A total of 467 parameters were refined: 58 instrumental/histogram terms and 409 structural parameters. For the two neutron data sets, 12 background parameters, a scale factor, two peak shape parameters and two/three instrument calibration constants were refined; for X-ray data, 12 background parameters, a scale factor, six peak shape parameters, a peak asymmetry correction, and a sample height correction were refined. An absorption correction was refined for both the X-ray and 90° neutron data. Structural parameters were three cell parameters, 402 coordinates, and four isotropic displacement parameters.

Structure Solution Methodology

Initial inspection of both X-ray and neutron powder data revealed that there was no obvious splitting of diffraction peaks to confirm the orthorhombic symmetry indicated by ^{31}P solid-state NMR measurements. Model-independent Pawley fitting[25] of individual data sets (see Figure 2) showed that better fits could be obtained in space group *Pbca* than $Pa\bar{3}$ suggesting that, despite no observable peak splitting, the data might contain information about the true metric symmetry of the cell in individual peak shape asymmetries. Neutron data over a time-of-flight range of 80 000−114 000 μs gave weighted profile *R*-factors (R_{wp}) of 6.83 and 2.15% in space groups $Pa\bar{3}$ and *Pbca*, respectively; X-ray data from 7 to 28° 2θ gave R_{wp} values of 7.21 and 5.74%. It should, however, be noted that the number of reflections used to fit the experimental data increases significantly on reducing the symmetry from 377 to 1127 and from 620 to 1998 for neutron and X-ray data sets, respectively, such that the improvement in fit may result mainly from improvements in fitting the true experimental peak shape. Application of a traditional Hamilton test to the improvement in R_{wp} values would lead one to conclude that the improvement in fit is not statistically significant given the large increase in the number of parameters used in the model.

The complexity of ZrP_2O_7 (NMR shows it has 136 crystallographically unique atoms) makes its solution from powder data challenging. An additional complication is that the powder data appear to contain little or only weak information about the metric symmetry of the material. As such unit cell determination (i.e., the subtle differences between pseudocubic *a*, *b*, and *c* dimensions) becomes part of the structure solution process, methods relying on extracted intensities of *hkl* reflections will fail. We have therefore adopted a direct space structure solution methodology in which many trial structural models are Rietveld refined simultaneously against neutron and X-ray data. Since there is a considerable body of literature information on materials containing ZrO_6 octahedra and P_2O_7 groups, it is also possible to include chemical restraints on constituent polyhedra during the structure solution process. The relative weights of distance/angles restraints were adjusted by performing data-independent distance-least-squares (DLS)[26] modeling using Topas Academic until bond distance/angle distributions were similar to those found experimentally in related materials in the ICSD.

To solve the structure, which requires a minimum of 405 independent structural parameters (3 cell parameters and 402 fractional coordinates), it is important to include as much of the diffraction data as possible during structure solution. This does, however, slow calculations and reduces the efficiency with which parameter space can be explored. Data ranges of 40 000−113 000 μs (0.829−2.343 Å) (neutron) and 2−57.7° (0.849−22.9739 Å) (X-ray) were employed which offered a reasonable compromise between speed of calculations and the inclusion of a reasonable amount of data. A number of different solution strategies were investigated. Our final method of choice was to combine rigid body methods of refinement with standard free atomic refinement. In this

(20) Coelho A. A. *TOPAS, General Profile and Structure Analysis Software for Powder Diffraction Data*, version 3.0; Bruker AXS: Karlsruhe, Germany, 2004; http://members.optusnet.com.au/~alancoelho/.
(21) Norberg, S. T.; Svensson, G.; Albertsson, J. *Acta Crystallogr., Sect. C: Cryst. Struct. Commun.* **2001**, *57*, 225.
(22) Brese, N. E.; O'Keeffe, M. *Acta Crystallogr., Sect. B: Struct. Sci.* **1991**, *47*, 192.
(23) Brown, I. D.; Altermatt, D. *Acta Crystallogr., Sect. B: Struct. Sci.* **1985**, *B41*, 245.
(24) Lister, S. E.; Evans, I. R.; Howard, J. A. K.; Coelho, A.; Evans, J. S. O. *Chem. Commun.* **2004**, 2540.
(25) Pawley, G. S. *J. Appl. Crystallogr.* **1981**, *14*, 357.
(26) Baerlocher, C.; Hepp, A.; Meier, W. M. *DLS-76*; Swiss Federal Institute of Technology (ETH): Zurich, Switzerland, 1976.

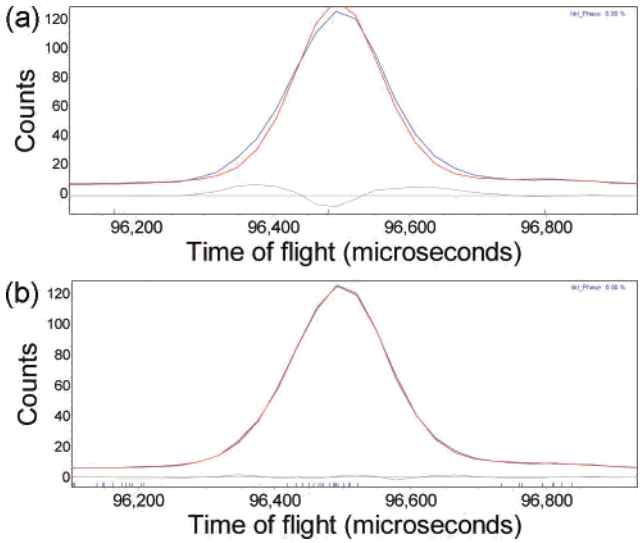

Figure 2. Pawley fits of the (0,3,12) reflection ($d \approx 2$ Å) of ZrP_2O_7 using (a) a cubic model in space group $Pa\bar{3}$ and (b) an orthorhombic model in space group *Pbca*. Allowed reflection positions are shown as small vertical tick marks.

method, structural models were initially described in terms of P_2O_7 rigid bodies free to move and rotate in three dimensions, free to bend their P−O−P bond, and having a free internal torsion angle. The P−O(−P) bond length was defined according to the P−O−P angle. These groups and Zr atoms were then displaced from ideal positions in a $3 \times 3 \times 3$ orthorhombic superstructure calculated from the simple high-temperature structure of Figure 1. Internal bond angles and torsion angles of P_2O_7 groups were set to random values between 120−180° and 0−120°, respectively (0 representing a fully eclipsed P_2O_7 group). Full Rietveld refinement was then performed (structural parameters, cell parameters, peak shape parameters, and background parameters were refined) using both neutron and X-ray data sets. After two cycles of refinement, the rigid P_2O_7 groups were automatically replaced by normal independent atoms, and coordinates were allowed to refine freely, though bond distance/angle restraints were retained. Following convergence, rigid bodies were reintroduced, cell parameters were reset to equal values, and the randomization process was repeated. The R_{wp} values typically varied from ∼40 to 6% during each randomization/refinement cycle. During structure solution stages the O_3P_a−O−P_aO_3 P_2O_7 group was treated as lying on a center of symmetry and therefore having a 180° P−O−P bond angle and a 30° torsion angle. Several thousand cycles of randomization/refinement were performed and the lowest R_{wp} refinements saved for further analysis.

Figure 3 shows a plot of the unit cell parameters and R_{wp} values obtained from 100 cycles of randomization/refinement. It can be seen that final R_{wp} values obtained ranged from ∼6.8% down to 5.9% showing that refinements do not always converge to the true structural minimum. In these attempts an *R*-factor less than 6% was obtained from 15% of the trial structures. It is interesting to note that the low *R*-factor solutions consistently have cell parameters in which $b < a \approx c$. This shows that, despite the lack of visible peak splitting, the data contain information about the true metric

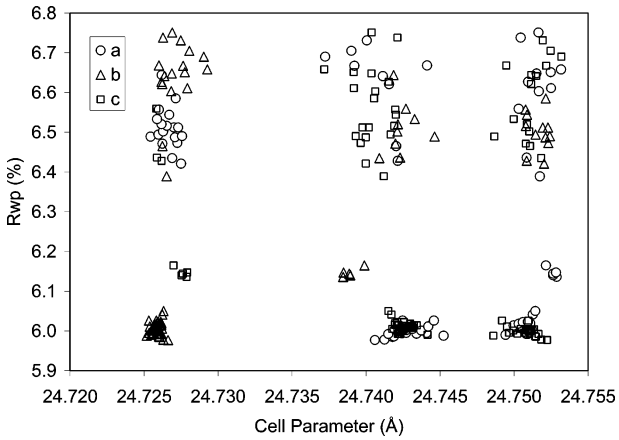

Figure 3. A scatter plot showing the R_{wp} values obtained and unit cell parameters for 100 trial cycles of randomization/convergence. Cell parameters *a*, *b*, and *c* are plotted as circles, triangles, and squares, respectively. The lowest R_{wp} solutions consistently have $b < a \approx c$; the range of values obtained gives an indication of the true precision to which cell parameters, which are correlated with structural parameters, can be determined.

Table 1. Rietveld Refinement Details[a]

	LT ZrP_2O_7	LT HfP_2O_7
a (Å)	24.7437(4)	24.652(2)
b (Å)	24.7258(3)	24.6296(6)
c (Å)	24.7507(4)	24.651(1)
V (Å^3)	15 177.0(3)	14 967.4(1)
R_{wp} (all/neutron/X-ray) (%)	5.99/3.83/7.80	4.79/1.85/2.08/11.53
R_{Bragg} (neutron/X-ray) (%)	2.16/3.11	0.89/0.93/4.00
no. reflns (neutron/X-ray)	21195/ 22015	18170/45774/11105
structural params	409	409
total params	446	467

[a] For HfP_2O_7, two banks of neutron data were used.

symmetry of the system in individual peak shapes. We note that even with the use of this limited data range, the values of cell parameters obtained of $a = 24.7406$, $b = 24.7266$, and $c = 24.7522$ Å show a similar splitting pattern to those obtained by Birkedal et al.[21] Coordinates of the 10 lowest R_{wp} solutions were compared and found to be essentially identical: the average shift of atoms in any one of these coordinate sets from the overall average was 0.022 Å; the largest shift was 0.12 Å. This confirms that the same structural minimum is consistently found using this protocol.

The best structure solution from the simulated annealing studies was used as the starting point for full Rietveld refinement. This used neutron data, from 0.7258 to 2.4343 Å (21 195 *hkl* reflections), and X-ray data from 0.7258 to 22.9739 Å (22 015 *hkl* reflections). During refinement the P−O(−P) distance of the O_3P_a−O−P_aO_3 group was allowed to be shorter than in other groups. Refinement gave a final R_{wp} of 5.985% and an R_{Bragg} of 2.16 and 3.11% for X-ray and neutron data, respectively. Final Rietveld plots are shown in Figure 4 and refinement details in Table 1. Histograms showing the range of bond distances and angles within ZrO_6 octahedra and PO_4 tetrahedra are shown in Figure 5.

The availability of the high quality single-crystal refinement of Birkedal et al. provides a valuable opportunity to assess the quality of structural refinements that can be achieved for a material of this complexity from powder data. Final cell parameters from our combined Rietveld refinement were $a = 24.7437(4)$, $b = 24.7258(3)$, and $c = 24.7507(4)$

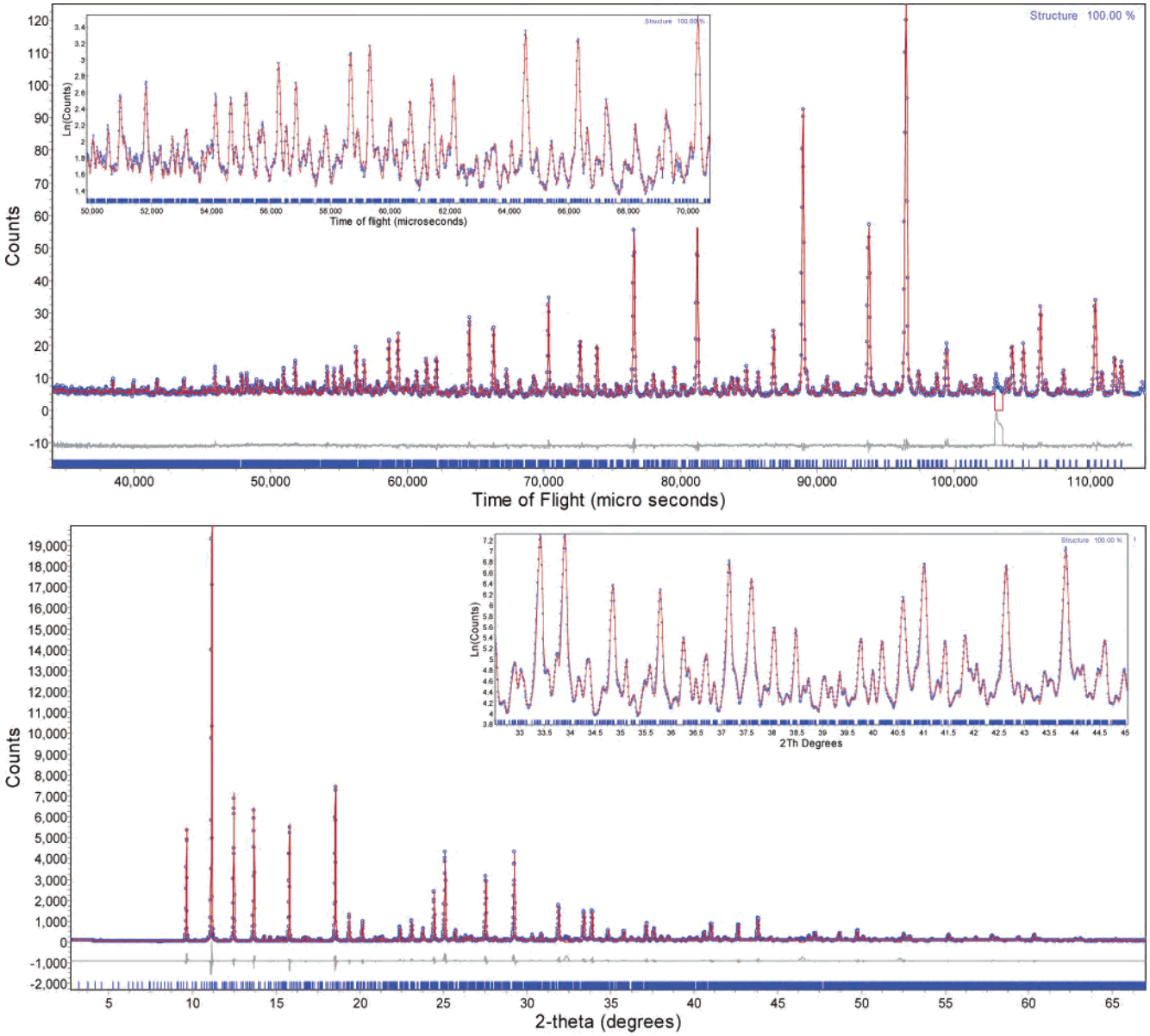

Figure 4. Final Rietveld plots for neutron and X-ray refinements. Inserts show zoomed regions corresponding to *d* spacing ranges of ~1.45 to 1.04 Å plotted on a logarithmic scale to emphasize the weak superstructure reflections. Observed data are shown as blue points, calculated data as a solid red line, and difference data as a lower gray line. Allowed peak positions are shown as small vertical tick marks.

Table 2. P−O−P Bond Angles (deg) for the 14 Independent P_2O_7 Groups[a]

P−O−P group	POP angle (single cryst)	POP angle (powder)	P−O−P group	POP angle (single cryst)	POP angle (powder)
2	145.0	143.7(9)	14	150.2	147.6
4	143.1	142.3(12)	6	147.2	146.8(12)
7	147.8	148.2(13)	13	152.4	148.3(12)
8	142.0	142.9(7)	1	146.4	143.4(5)
10	145.9	147.9(6)	3	145.0	147.3(12)
11	140.7	141.0(11)	5	143.3	142.3(12)
12	144.4	143.6(13)	9	145.7	143.2(12)

[a] For P_2O_7 group 14, which has a disordered P_2O_7 group modeled here with a 180° bond angle, the true local bond angle has been estimated from the refined length of the P−O(−P) bonds compared to those of other groups.

Å which show a departure from their average value (24.7400 = 3 × 8.2466 Å) of −0.015, 0.058, and −0.043%. These compare to values of a = 24.7390(2), b = 24.7184(2), and c = 24.7431(2) Å which show a departure from their average value (24.7335 = 3 × 8.2445 Å) of −0.022, 0.061, and −0.039% for the crushed single crystal used by Birkedal et al. Clearly our powder data, despite not showing clear peak splitting, allow the true metric distortions of the sample to be determined reliably. The absence of splitting could be due to the lower resolution of our X-ray data; however, we note that the neutron data showed a clear sample contribution to the overall peak shape. Comparison of the two structures shows that coordinate shifts between them are extremely small. Excluding the oxygen of the disordered phosphate group, the average shift between atomic coordinates for the two refinements was 0.056 Å; the range of shifts is shown in Figure S1. We note that a shift in a typical O atom by 1 standard uncertainty in *x*/*y*/*z* from the powder refinement would correspond to a distance of ~0.035 Å. Selected

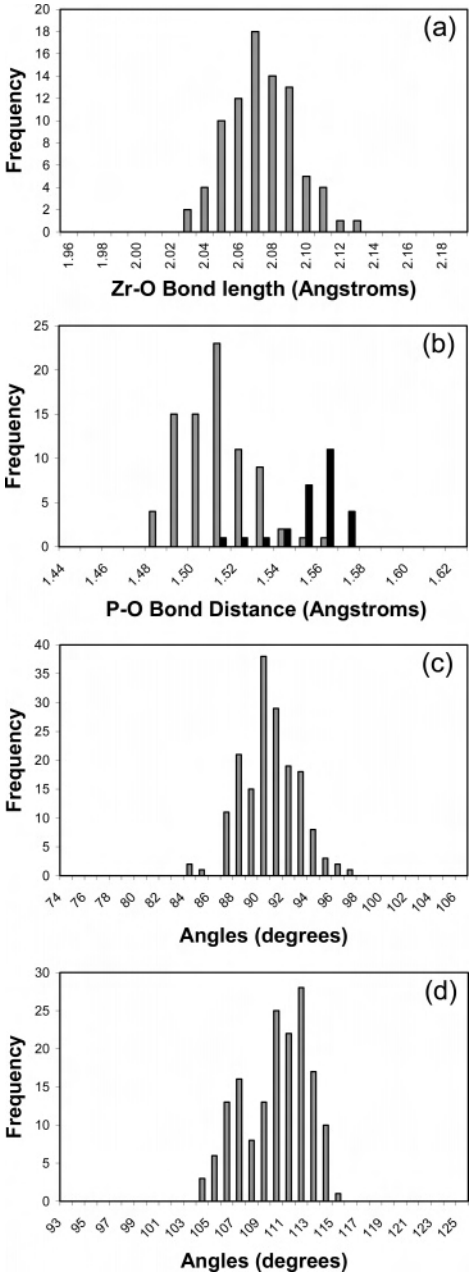

Figure 5. Histograms showing the distributions of (a) Zr−O distances, (b) P−O distances with P−O(−P) shaded black, (c) O−Zr−O 90° angles, and (d) P−O−P tetrahedral angles.

sections of the structure are shown along with a comparison of selected P_2O_7 groups in Figure 6. Table 2 and Figure 6 show that both the P−O−P bond angles and torsions of individual groups are well determined from the powder data. A superposition of all P_2O_7 groups from powder and single-crystal refinements (equivalent to Figure 4 in Birkedal et al.'s paper) is included in the Supporting Information, Figure S2. Average bond lengths and standard deviations for Zr−O, P−O(−Zr), and P−O(−P) in our refinements are 2.069(0.020), 1.503(0.016), and 1.567(0.016) Å, respectively, compared to 2.058(0.012), 1.504(0.006), and 1.574(0.007) Å as reported by Birkedal et al. The powder data clearly allow a precise refinement of the true structure of ZrP_2O_7.

To show the improvement in fitting the powder data in

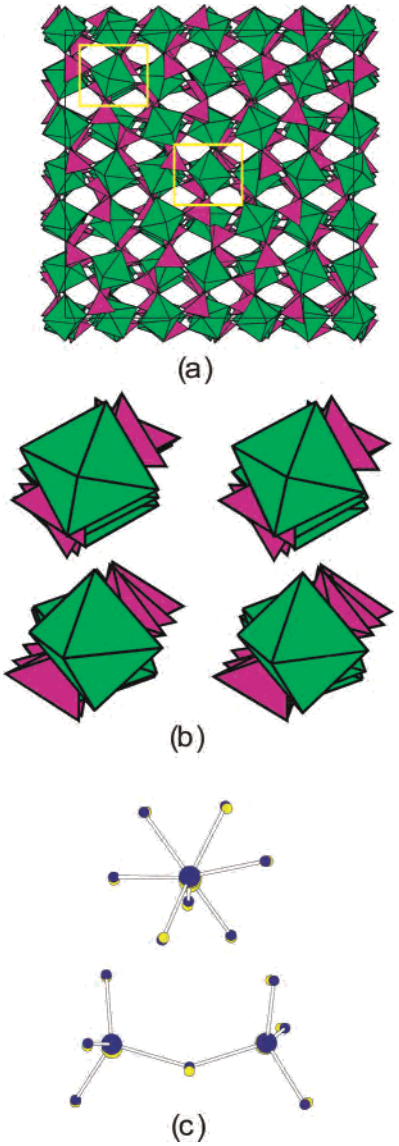

Figure 6. (a) A polyhedral view of the superstructure of ZrP_2O_7 from powder refinements; (b) a zoom of two regions of the powder structure (left) and a comparison to equivalent regions of the single-crystal structural refinement (right); (c) a superposition of atoms from a typical P_2O_7 group from powder (light) and single-crystal (dark) refinements.

Pbca as opposed to $Pa\bar{3}$ (as reported previously) is real, we have also performed our structure solution and refinement strategy in space group $Pa\bar{3}$. Polyhedral distances and angles were restrained to adopt a similar spread of values to the *Pbca* refinements. A total of 100 separate randomization/refinement cycles equivalent to those in Figure 3 gave R_{wp} values between 8.55 and 10.37%. Rietveld plots of the best results are compared to those in *Pbca* in Figure 7. Application of a Hamilton test based on R_{wp} values indicates that the improvement in fit obtained in *Pbca* is statistically significant.

Rietveld refinement of the structure of HfP_2O_7, which has also been shown to be orthorhombic by ^{31}P solid-state NMR,[27] has been performed using the ZrP_2O_7 structure as a

(27) King, I. J. Ph.D. Thesis, University of Durham, Durham, U.K., 2003.

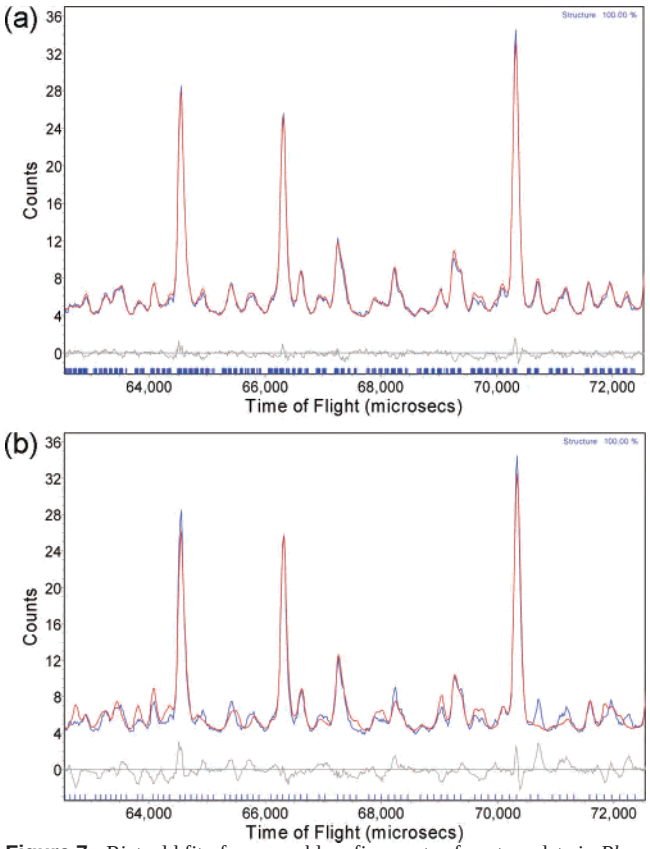

Figure 7. Rietveld fit of comparable refinements of neutron data in *Pbca* (a) and $Pa\bar{3}$ (b). Experimental data are shown in blue, fit data in red, and the difference in gray. Tick marks below the data are positions of *hkl* peaks.

starting point. Rietveld plots are included in the Supporting Information, Figure S3. Final coordinates showed an average shift of 0.0693 Å (based on the cell parameter of ZrP_2O_7) from those of ZrP_2O_7 showing that the two materials are isostructural. Cell parameters of $a = 24.652(2)$, $b = 24.6296(6)$, and $c = 24.651(1)$ Å showed a departure from their average value ($24.6441 = 3 \times 8.2147$ Å) of −0.032, 0.060, and −0.028%, similar in magnitude to those in ZrP_2O_7.

Conclusion

Despite their structural complexity the 136-atom structures of ZrP_2O_7 and HfP_2O_7 have been solved from powder diffraction data using a direct space approach applied to a combination of X-ray and neutron data. The data are consistent with relatively undistorted ZrO_6/HfO_6 and PO_4 tetrahedra with 13 of the 14 crystallographically unique P_2O_7 groups adopting a P−O−P bond angle between 141 and 149°. One group lies on a center of symmetry, but the P−O(−P) bond distances indicate it is disordered over two configurations and has a bond angle similar to that of other groups.

Acknowledgment. We would like to thank Pat Woodward for collecting the synchrotron data set and the Engineering and Physical Sciences Research Council (EPSRC) for funding and access to neutron facilities. We would like to thank Richard Ibberson, Richard Gover, and Clare Crossland for assistance in collecting diffraction data.

Supporting Information Available: Figures showing the atomic displacements between powder and single-crystal refinements, superpositions of all independent $P_2O_7^{4-}$ groups, and Rietveld plots for HfP_2O_7. This material is available free of charge via the Internet at http://pubs.acs.org.

IC060016B